



COMPARISON OF DIFFERENT CONTROL STRATEGIES FOR A DIRECT DRIVE PMSG BASED GRID INTEGRATED WIND ENERGY CONVERSION SYSTEM

¹Sajan.CH, ²Sagar.E, ³Kalyani.P, ⁴Sreenidhi.T

¹Associate Professor, ^{2,3,4}UG Students

^{1,2,3,4}Department of Electrical and Electronic Engineering,

^{1,2,3,4}Jyothismathi Institute of Technology and Science, Karimnagar, Telangana, India

Abstract : Future projections suggest that a growing proportion of the world's energy will come from wind power. Nevertheless, since wind power gets more widespread in the grid, new worries about system reliability and stability emerge. As a result, there are now more opportunities to enhance power quality and create control systems that support the grid during voltage disruptions. This study proposes a comparison between PI, SMC and ANFIS approach for a direct drive PMSG wind energy change framework. Nonlinear Sliding Mode Control (SMC) is an amazing strategy for dealing with lattice unsettling influences because of its sturdiness and high aggravation dismissal capacities. The SMC chattering effect increases the overall harmonic distortion that is added to the grid. This work effectively reduces the SMC demerit by carefully selecting of a controller and its dynamics from the ANFIS control law design. MATLAB/Simulink simulation findings demonstrate that the recommended control scheme performs significantly compared to the obviously changed relative basic control during lattice voltage blackouts.

IndexTerms - GSC Control, MSC Control, Permanent Magnet Synchronous Generator, Artificial Neuro Fuzzy Inference System Control, Wind Energy.

I. INTRODUCTION

Wind energy has filled in fame throughout the course of recent a very long time as a carbon-nonpartisan environmentally friendly power source. A variable breeze speed turbine might be designed to stumble into a wide speed reach to expand the power created by the breeze. Long-lasting magnet simultaneous generators, or PMSGs, are progressively seen in direct-drive turbines. PMSGs generate more power per unit area and are more efficient than wrapped rotor generators. employed to minimize mechanical stress brought on the speed multiplication (gear box) in order to maximize energy extraction, improve system reliability, and save maintenance costs [1].

The modern wind turbines that they allow to operate at variable speeds produce more electricity than those that are set at a constant speed [1-2]. It may be difficult to manage the electrical generator when utilizing a wind turbine because the wind speed influences the turbine's rotating speed.

After examining a number of wind turbine designs, researchers discovered that those using asynchronous motors were more affordable and required less upkeep. However, managing their velocity necessitates more complex and expensive power electronics apparatus. the third [4]. The sacred goal of wind energy frameworks is greatest power proficiency and, in this manner, the ability to utilize the breeze to its fullest. For this situation, the MPPT control is very significant. There are multiple ways of keeping the effectiveness working point at its pinnacle. Ideal power/force following is the most frequently utilized control technique [5]. Traditionally, the proportional and integral controller approach is implemented [5]. However, this strategy won't provide better outcomes. This problem could be solved by other control strategies including sliding mode control and fuzzy logic [6]. Because of the way its control variables are structured, sliding mode control is a non-linear control.

Since its presentation in the mid-1950s, control issues have been really settled with it. It is impervious to framework vulnerabilities and disturbances from an external perspective as well as within. This control's credits incorporate high accuracy, quick unique reaction, security, and straightforwardness in plan and execution. [6]

This article intends to give a severe control to get better execution. The paper's blueprint is as per the following analyses the WECS. Eventually, the reenactment's discoveries approve the viability of the suggested approach, and the proportional and integral (PI), sliding mode control (SMC) and Artificial neuro fuzzy inference system (ANFIS) configuration is done. In the MATLAB/Simulink climate, the suggested technique outflanks regular PI regulators.

II. MACHINE SIDE CONTROLLER SCHEME

PMSG Model the permanent magnet synchronous generator's mathematical model is provided in this subsection; all values are given in terms of units.

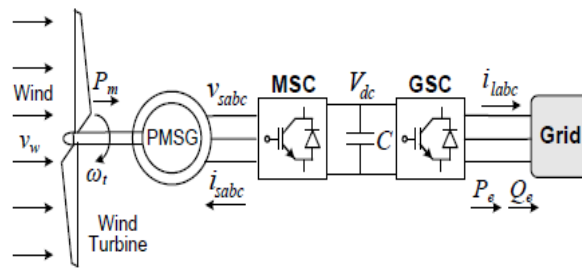


Fig. 1. Configuration of a direct-drive PMSG wind turbine

The static voltage for the PMSG as its component within the d-q frames can be expressed as: The variables v_d and v_q indicate the stator voltages on the dq-axis, while i_{ds} and i_{qs} indicate the stator currents on the dq-axis. L_d and L_q refer to the reactance of the stator on the dq-axis. ψ_f symbolizes the peak flux of the permanent magnet synchronous generator (PMSG), while R_s represents the resistance of the stator winding. ω_r represents the electrical speed of the rotor, and ω_{base} is the base electrical speed of the PMSG.

$$\begin{bmatrix} v_d \\ v_q \end{bmatrix} = \begin{bmatrix} R_s & -\omega_r L_q \\ \omega_r L_d & R_s \end{bmatrix} \begin{bmatrix} i_{ds} \\ i_{qs} \end{bmatrix} + \begin{bmatrix} L_d/\omega_{base} & 0 \\ 0 & L_q/\omega_{base} \end{bmatrix} \frac{d}{dt} \begin{bmatrix} i_d \\ i_q \end{bmatrix} + \begin{bmatrix} 0 \\ \omega_r \psi_f \end{bmatrix} \tag{1}$$

The electromagnetic torque can be obtained using:

$$T_e = [\psi_f i_q + (L_d - L_q) i_d i_q] \tag{2}$$

For the PMSG $L_d=L_q=L$, therefore (2) may be reduced as:

$$T_e = \psi_f i_q \tag{3}$$

The behavior of the generator is illustrated as:

$$2H \frac{d}{dt} \omega_m + B \omega_m = T_e - T_m \tag{4}$$

where, T_e and T_m stand for the electromagnetic and mechanical torques, respectively, and inertia time constant is denoted by H, viscous friction by B, and rotor mechanical speed by ω_m .

Lattice side converter control is at times used to address for music as well as to change the voltage across the DC association. This two-stage regulator method is achieved by adjusting the dq-hub toward the lattice voltage, or by utilizing a vector control conspire that is centered around matrix voltage.

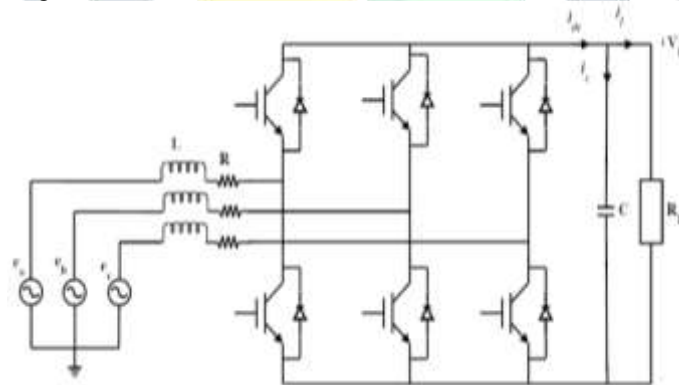


Fig. 2. Converter Configuration

A network side converter circuit that draws power from a fair three-stage circuit is found in the above graph. This converter utilizes an IGBT switch and is a voltage source converter. The channel capacitor C in the outline feeds to the heap obstruction R, making up the DC connect. The essential objective of grid converter to keep a consistent DC connect voltage; if necessary, it can likewise give a limited quantity of responsive power.

III. GRID SIDE CONTROLLER SCHEME

Grid-connected converters are power electronic devices that link energy storage systems, flexible loads, and energy from renewable sources to the electric grid. They may provide a number of advantages, including active filtering, frequency support, voltage adjustment, and improved power quality. However, since it entails a number of goals and trade-offs, creating a control strategy for a grid-connected converter is not an easy operation.

The grid-based converter control includes 2 loops of control. The operational mechanism of GSC follows the structure mentioned below.

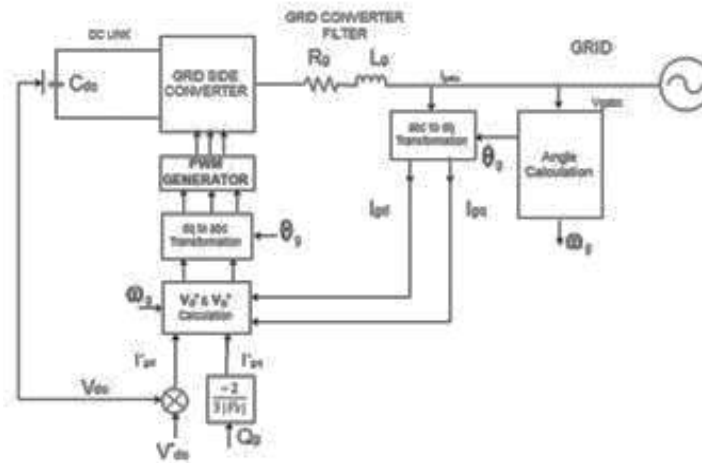


Fig. 3. Vector control of grid side controller

A few important topics of grid-connected converter control that will be covered in this article include grid synchronization, power control, current control, and modulation approaches.

A. Grid synchronization

Synchronizing the converter with grid voltage and frequency is one of the initial stages in grid-connected converter control. This is necessary to minimize power losses and harmonics and to provide steady and dependable operation. Grid synchronization may be achieved by a variety of techniques. The grid circumstances, converter topology, and application requirements all influence the technique selection. For instance, since PLL can precisely measure the grid phase angle and frequency, it is often employed for single-phase or three-phase converters. Due to its ability to convert grid voltages into a rotating reference frame, SRF is appropriate for three-phase converters operating on either balanced or unbalanced grid voltage. However, as both approaches are often used in their operations, PLL and SRF are not always separate procedures. Droop control is a decentralized technique that modifies the frequency and voltage in accordance with the active and reactive power, allowing many converters to be coordinated without the need for communication.

B. Power control

Controlling the amount of both active and reactive power exchanged with the grid is another crucial component of grid-connected converter control. Either the converter output current magnitude and phase angle or the converter output voltage magnitude and phase angle may be adjusted to accomplish this. The grid connection point, the control goals, and the converter operating mode determine the power control approach. For instance, the converter could have to function as a voltage source and maintain a steady voltage magnitude and frequency at the point of common coupling (PCC) if it is coupled to a weak grid or a micro grid. In order to meet grid demand or take advantage of renewable energy sources, the converter may need to function as a current source and inject or absorb active and reactive power if it is linked to a robust grid or transmission system.

C. Current control

Since it controls the quality and stability of the converter output current, current control is an essential part of grid-connected converter control. A variety of techniques, including hysteresis control, may be used to accomplish current control. The grid impedance, harmonic performance, and converter switching frequency all influence the choice of current control technique. Hysteresis control, for instance, is a quick and easy way to turn the converter on and off based on a preset current error band. High switching losses and variable switching frequency might result from it, however. PI control is a widely used and reliable technique that uses feedforward and feedback terms to control the current error to zero. It could, however, have issues with steady-state errors and function poorly when there are distortions in the grid. PR control adds resonant terms at the grid frequency and its multiples, improving harmonic rejection and eliminating steady-state errors in comparison to PI control. Using a predictive model of the converter and the grid, MPC is a sophisticated technique that can optimize the converter switching states.

D. Modulation techniques

The processes known as modulation techniques are what produce the converter's switching signals in accordance with the intended output voltage or current. They may have an impact on dynamic responsiveness, harmonic distortion, and converter efficiency. Grid-connected converters may be modulated using a variety of methods. The harmonic spectrum, switching frequency, and converter structure all influence the modulation method selection. For instance, PWM is a popular and straightforward method that may change the switching signals' duty cycle in response to both a carrier and a reference signal. At low switching frequencies, it can, nonetheless, result in significant harmonic distortion and switching losses. The position of the reference vector in a space vector diagram may be used to produce switching signals using SVM, a more flexible and efficient method. It could, however, call for more sophisticated algorithms and computer power. SHE is an advanced method that works by solving a series of nonlinear equations to remove certain harmonics. It could, however, only be partially applicable and have stability problems.

IV. ANFIS CONTROLLER

ANFIS, which is an integration of two distinct soft-computing techniques: ANN with Fuzzy Inference System, that was initially developed by Jyh-Shing Roger Jang in the year 1992. It operates within the Sugeno fuzzy inference framework as its

architecture resembles to the multilayered feedforward neural network structure, with the exception that the connections in ANFIS represent the communication' flow direction whereas there aren't any associated weights for those links. Fig. 4 depicts the Sugeno fuzzy model that includes two rules together with the associated ANFIS framework.

To make easier that idea, a pair of rules in the way of "If-Then" in the Sugeno model are going to be considered using the two variables x and y for inputs with f as output.

The ANFIS structure is expressed using two fuzzy if-then rules based on the Takagi Sugeno (TS) model:

Rule 1: If (x is A_1) and (y is B_1) then $f_1 = p_1x + q_1y + r_1$

Rule 2: If (x is A_2) and (y is B_2) then $f_2 = p_2x + q_2y + r_2$

Figure-5 displays the complete block diagram that illustrates the ANFIS controller approach designed to deal with a two-rule fuzzy system. Takagi Sugeno (TS) rules are implemented in five levels by the ANFIS controller system via the employment using a mixed learning algorithms & a multi-iteration learning approach.

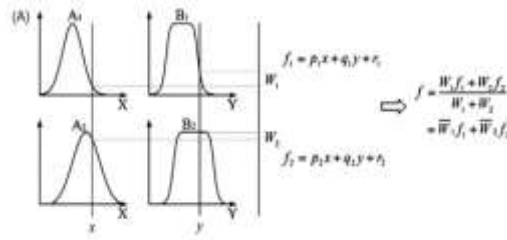


Fig. 4. Sugeno fuzzy model

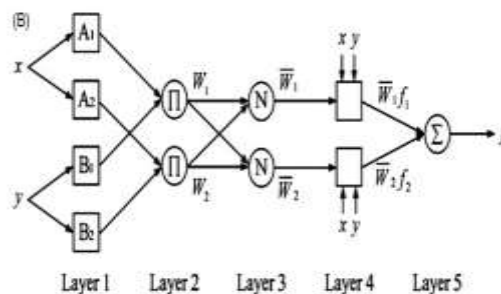


Fig. 5. Equivalent ANFIS architecture

The goal of this research is to propose a unique architecture termed Adaptive-Network-Based Fuzzy Inference System (ANFIS), from this perspective. This design can also be utilized as a base to develop a database of fuzzy rule sets with adequate membership functions in order to produce the intended input-output pairs.

V. RESULTS AND ANALYSIS

To accomplish the advantages of proposed system by modulating and simulating in MATLAB. All the three configurations of PI, SMC and ANFIS has been implemented.

A. Step Change in Wind Speed

As the wind speed fluctuates at the time intervals of 5,10,15sec then the systems lead to temporary disturbances in link voltage. This, in turn, affects the produced active power, resulting in a little decrease as seen in Figure 8. The suggested control approach exhibits reduced magnitude fluctuations in contrast with the standard PI and SMC methods during transients. Figure 10 illustrates the rotational velocity of the Permanent Magnet Synchronous Generator (PMSG).

All control methods have successfully attained satisfactory reference tracing capabilities. Nevertheless, a marginal discrepancy arises among the standard and actual speeds due to the PI and SMC control of a three-phase grid currents at Bus 5. The magnitude of those electrical currents correlates to a change in wind speed.

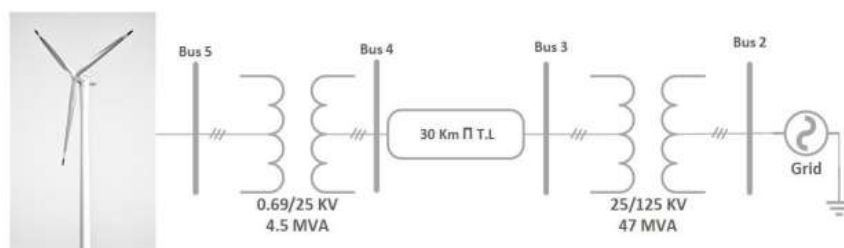


Fig. 6. Single line model of a system

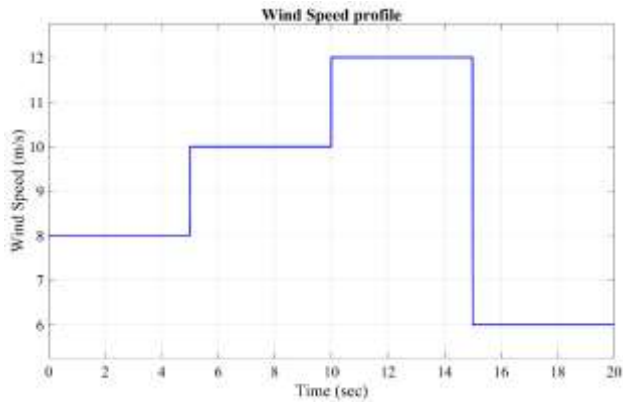


Fig. 7. Profile of input wind speed

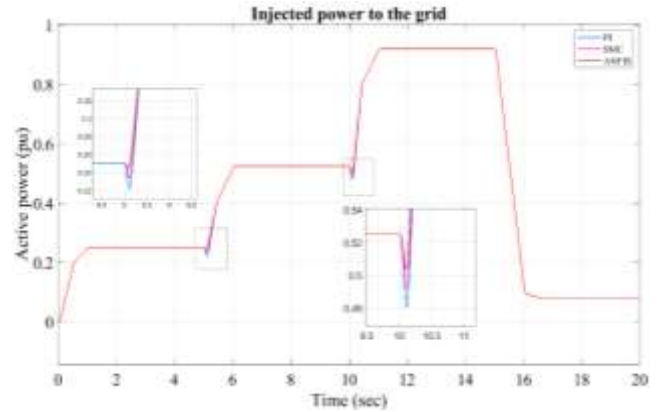


Fig. 8. Injected power to the grid

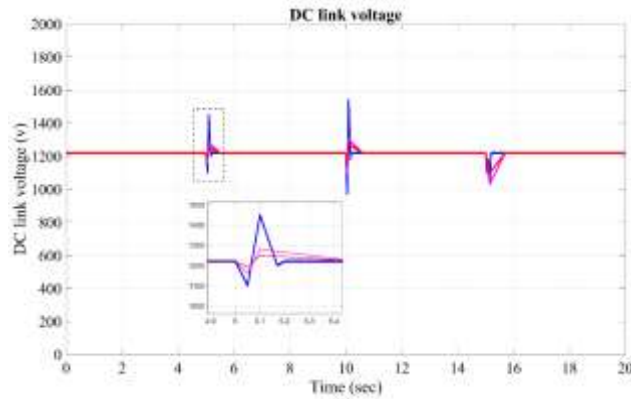


Fig.9. DC link Voltage

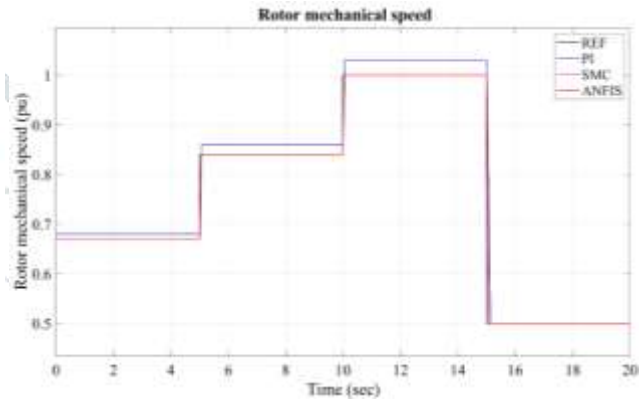


Fig. 10. Mechanical speed of rotor

B. THD Analysis

The system was emulated for a period of five seconds in order to determine the THD of grid currents, with steady-state results shown in Table 1. In comparison to the traditional PI control approach and SMC approaches, the THD of the suggested ANFIS control method is lower. and SMC approaches.

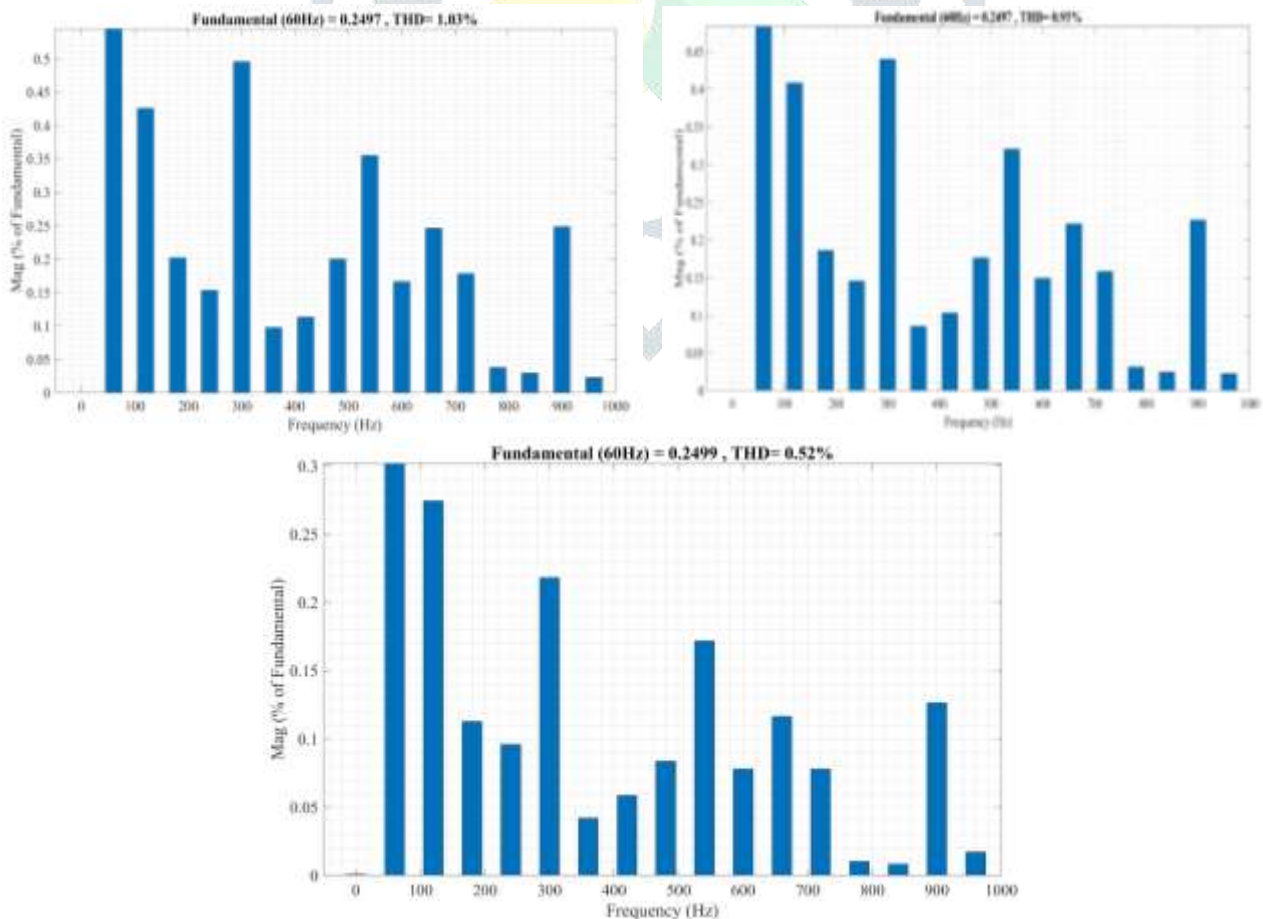


Fig. 11. THD levels with PI, SMC and ANFIS controller

Table 1. Comparative analysis

CONTROLLER	THD %
PI	1.03
SMC	0.93
ANFIS	0.52

C. Low-Voltage and High-Voltage Ride Through Capability

A three-phase voltage, which includes both active and reactive power that is injected into the grid, is depicted in Figure-12. Additionally, the voltage at the DC link is shown when a three-phase voltage drop of one hundred percent is provided to the system. When there is a disturbance in the grid voltage, the wind turbine continues to supply active power. This generates a discrepancy between the active power that is produced and the active power that is sent to the grid. As a result of this mismatch, the DC-link voltage quickly increases as a consequence of the imbalance. However, the ANFIS Controller technique has a greater transient response of DC-link voltage during the disturbance than both the PI and SMC methods. This is the case even if the PI method is also superior.

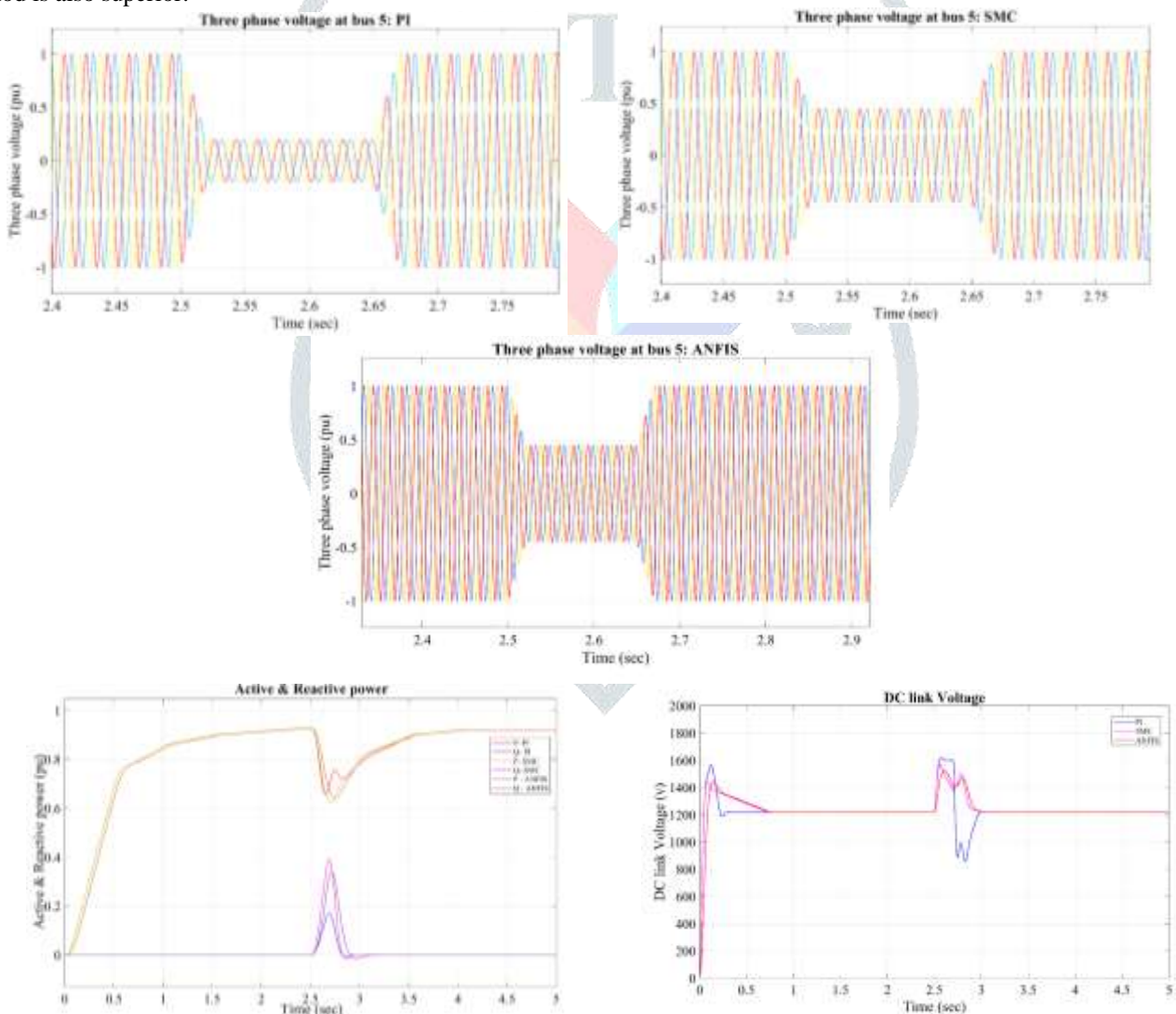


Fig.12. 100% of voltage dip - Three-phase voltage at Bus 5, Active and reactive power, DC link voltage with PI ,SMC & ANFIS controllers.

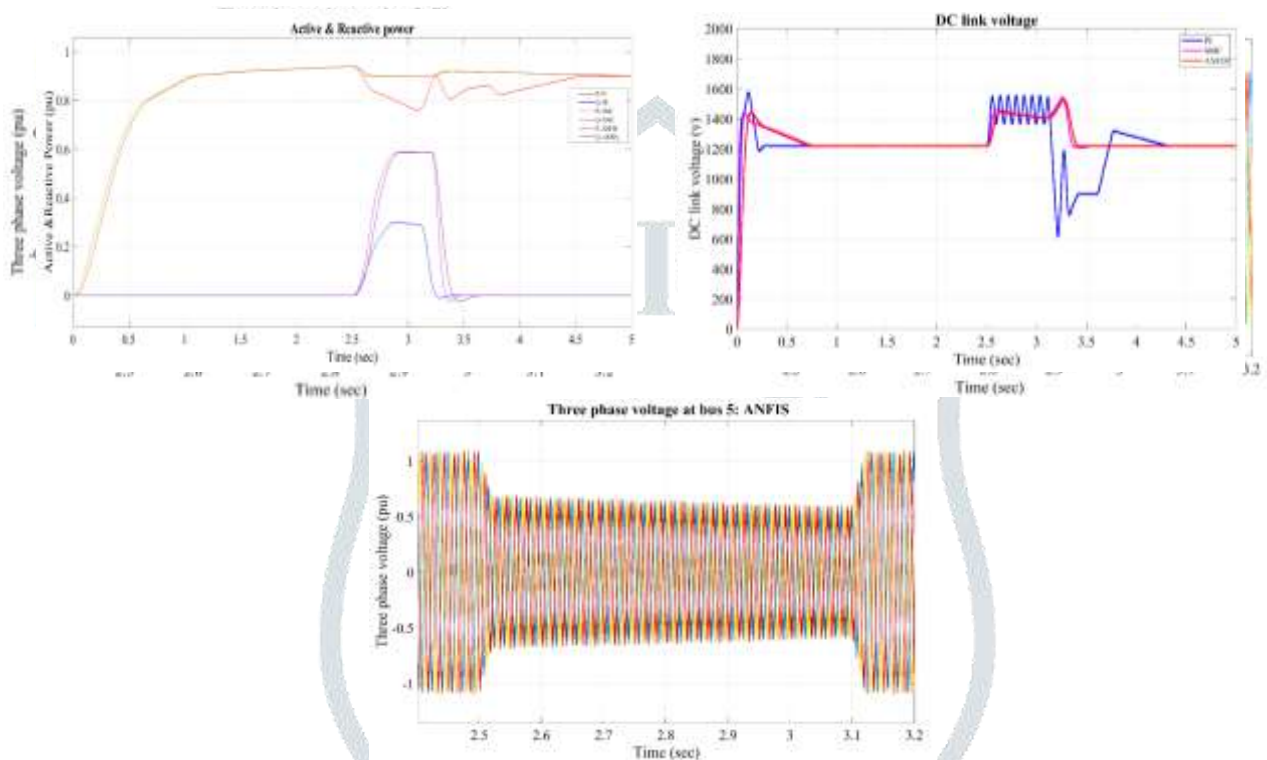
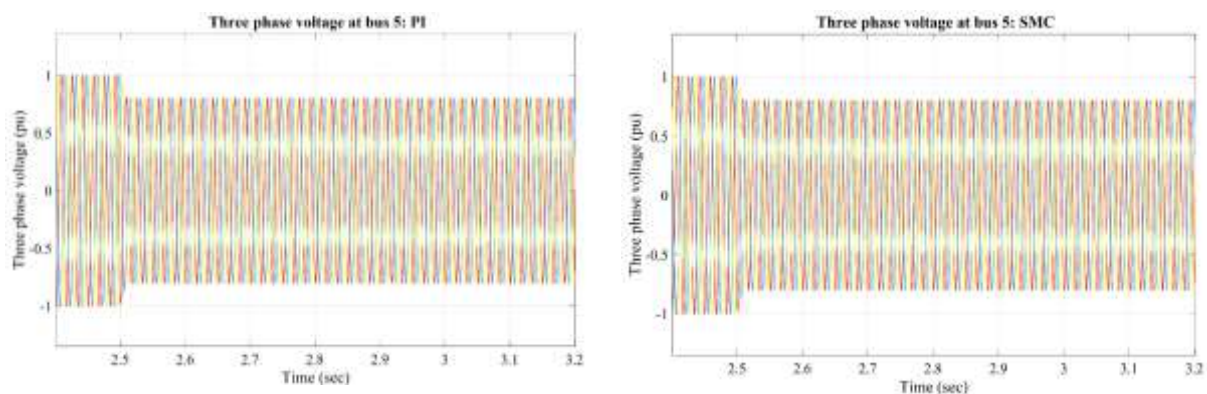


Fig. 13. 70% voltage dip- Three-phase voltage at Bus 5, Active and reactive power, DC link voltage with PI ,SMC & ANFIS controller.



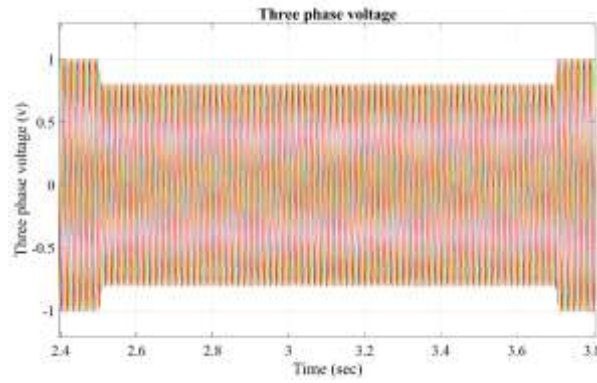


Fig. 14. 20% voltage dip- Three-phase voltage at Bus 5, Active and reactive power, DC link voltage with PI ,SMC & ANFIS controller.

Figure-13 displays the system's functioning while a 70% voltage decrease happened. The resulting powered wave is better and contains fewer variations comparable with the PI shown above.

It is also noteworthy that although little disruption happens, i.e., at the instance of the 20% decrease in voltage displayed in Figure 14, the short-term responses of the direct current, or DC, voltage, active, and reactive power of all of the control techniques are near However, when a major disruption occurs, the recommended control system's responsiveness outperforms that of the PI and SMC.

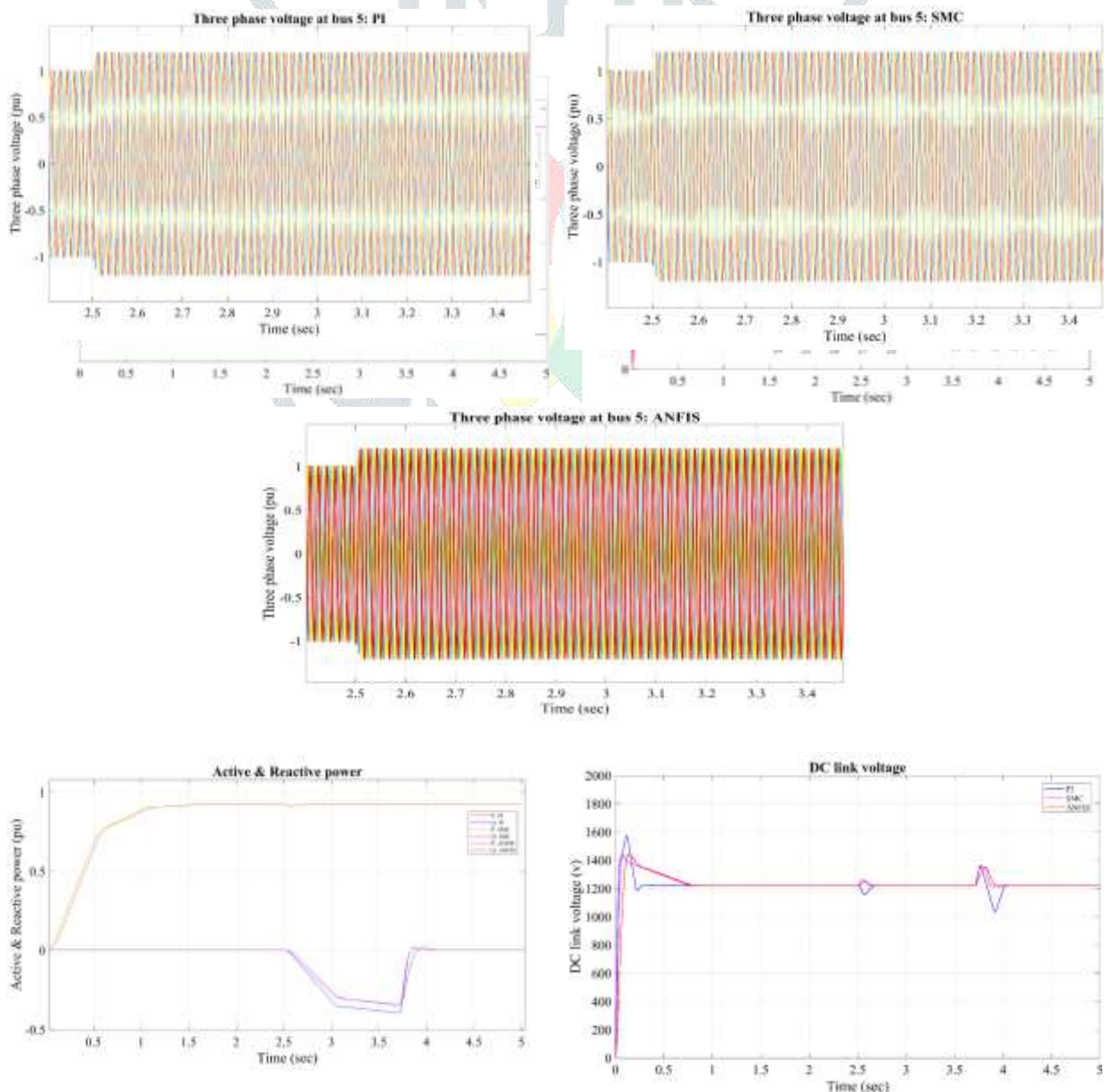


Fig. 15. 120% voltage swell- Three-phase voltage at Bus 5, Active and reactive power, DC link voltage with PI ,SMC & ANFIS controller

Figure-15 displays system functioning while the voltage across the grid arrives at 1.2 pu, in the scenario above the reactive power has been taken in through the grid.

D. Impact of Parameters Change and Model Uncertainty

There is also noise and instability in the parameters mentioned in the framework in order to further explore the analysis of the performance of the idea put forward fix. As an additional point of interest, the measurement of wind speed is vulnerable to random noise within the range of ± 0.5 meters per second.

Figures 16 through 19 illustrate the influence of parameter changes and the unpredictability of the model on the rotor's mechanical speed, electromagnetic torque, and voltage at the link. This is based on the assumption that the starting speed is 0.67 pu.

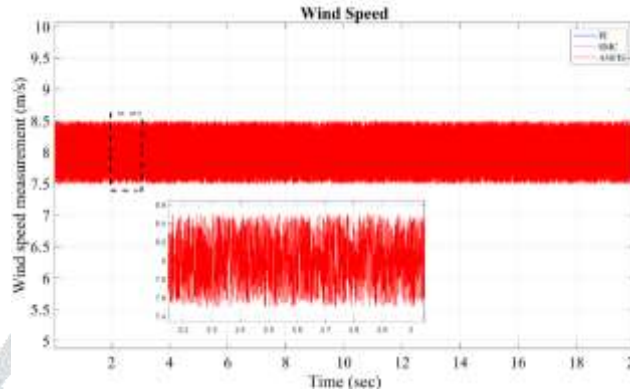


Fig. 16. Output waveforms of Wind Speed with PI,SMC and ANFIS controllers

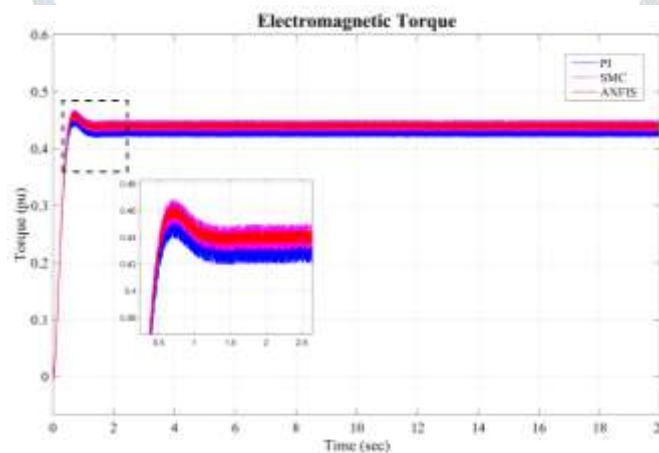


Fig. 17. Output waveforms of Electromagnetic Torque with PI,SMC and ANFIS controllers

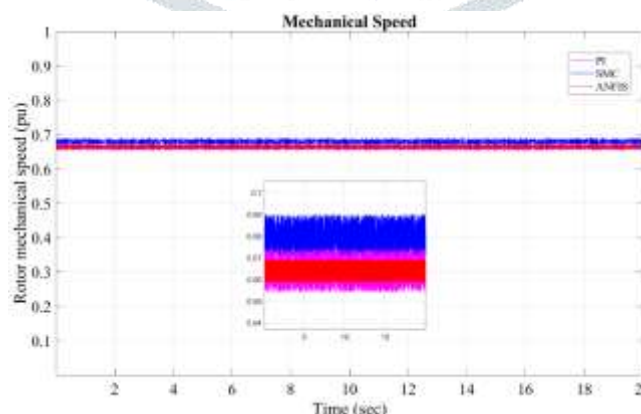


Fig. 18. Output waveforms of Mechanical Speed with PI,SMC and ANFIS controllers

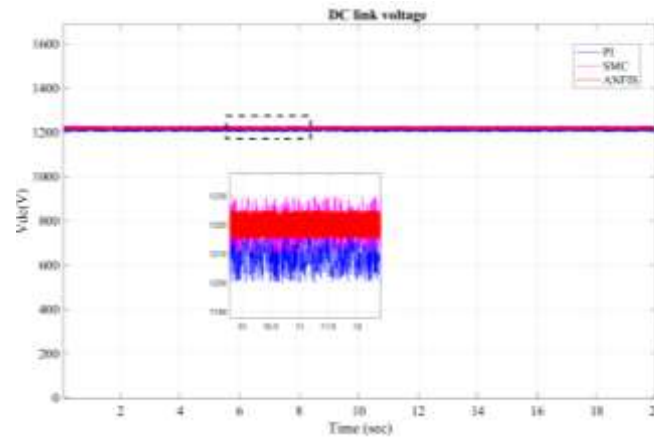


Fig. 19. Output waveforms of DC link voltage with PI, SMC and ANFIS controllers

It should be noted that the system that was suggested has maintained the rotor's speed at a value that is close to its optimal value. There is not a significant impact on the reaction time, as seen in Figure 17, which may be found here. Nevertheless, the noise measurement that is sent to the system causes the voltages at the DC link to fluctuate more than they would otherwise.

VI. CONCLUSIONS

This work has successfully constructed an ANFIS to handle the control of the wind system. A pitch control strategy for the PMSG turbine systems is suggested for limiting the rotation speed of turbine and maintain their power output at their specifications. In order that system reliability may be assured. The efficiency of the SMC scheme is validated by numerical simulations for fault scenarios in addition to for typical operational circumstances, and its characteristics are highlighted in comparison with standard Proportional Integral (PI) method of control as well as ANFIS Methodology. Based on the findings of the simulation, it is clear that the approach that was provided is effective, and the performance of the control system is satisfactory. The results achieved in the study are stated in the following order.

- (i) The effective building of the interactive mathematical framework of WES.
- (ii) The effective implementation of controllers to enhance operation during conditions of fault in addition to for typical usage.
- (iii) The dc link voltage can be well managed to assure dependable operation for the power electrical devices.

REFERENCES

- [1] Ahmed m. Osman, fahad alsokhiry, "Sliding mode control for grid integration of wind power system based on direct drive PMSG," volume 10, 2022 26567-26579 March 14, 2022.
- [2] K.-C. Tseng and C.-C. Huang, "High step-up high-efficiency interleaved converter with voltage multiplier module for renewable energy system," *IEEE Trans. Power Electron.*, vol. 61, no. 3, pp. 1311–1319, Mar. 2014.
- [3] H. Armghan, M. Yang, A. Armghan, and N. Ali, "Double integral action based sliding mode controller design for the back-to-back converters in grid-connected hybrid wind-PV system," *Int. J. Electr. Power Energy Syst.*, vol. 127, May 2021, Art. no. 106655.
- [4] V. Khare, S. Nema, and P. Baredar, "Solar–wind hybrid renewable energy system: A review," *Renew. Sustain. Energy Rev.*, vol. 58, pp. 23–33, May 2016.
- [5] Renewable capacity statistics 2020 International Renewable Energy Agency, IRENA, Abu Dhabi, United Arab Emirates, 2020.
- [6] M. E. Haque, M. Negnevitsky, and K. M. Muttaqi, "A novel control strategy for a variable-speed wind turbine with a permanent-magnet synchronous generator," *IEEE Trans. Ind. Appl.*, vol. 46, no. 1, pp. 331–339, Jan./Feb. 2010.
- [7] F. E. Tahiri, K. Chikh, and M. Khafallah, "Designing a fuzzy-PI controller of a stand-alone wind energy conversion system for MPPT," *Innovations in Smart Cities Applications Edition 2*. Cham, Switzerland: Springer, 2019.
- [8] Y. Errami, M. Hilal, M. Benchagra, M. Maaroufi, and M. Ouassaid, "Nonlinear control of MPPT and grid connected for wind power generation systems based on the PMSG," in *Proc. Int. Conf. Multimedia Comput. Syst.*, May 2012, pp. 1055–1060.
- [9] H. Polinder, F. F. A. van der Pijl, G.-J. de Vilder, and P. J. Tavner, "Comparison of direct-drive and geared generator concepts for wind turbines," *IEEE Trans. Energy Convers.*, vol. 21, no. 3, pp. 725–733, Sep. 2006.
- [10] J. Yan, H. Lin, Y. Feng, and Z. Q. Zhu, "Control of a grid-connected direct-drive wind energy conversion system," *Renew. Energy*, vol. 66, pp. 371–380, Jun. 2014.
- [11] M. Chinchilla, S. Arnaltes, and J. C. Burgos, "Control of permanentmagnet generators applied to variable-speed wind-energy systems connected to the grid," *IEEE Trans. Energy Convers.*, vol. 21, no. 1, pp. 130–135, Mar. 2006.
- [12] I. Munteanu, S. Bacha, A. I. Bratcu, J. Guiraud, and D. Roze, "Energyreliability optimization of wind energy conversion systems by sliding mode control," *IEEE Trans. Energy Convers.*, vol. 23, no. 3, pp. 975–985, Sep. 2008.
- [13] Y. Yang, K.-T. Mok, S.-C. Tan, and S. Y. R. Hui, "Nonlinear dynamic power tracking of low-power wind energy conversion system," *IEEE Trans. Power Electron.*, vol. 30, no. 9, pp. 5223–5236, Sep. 2015.
- [14] B. Zigmund, A. A. Terlizzi, X. del Toro García, R. Pavlanin, and L. Salvatore, "Experimental evaluation of pi tuning techniques for field-oriented control of permanent magnet synchronous motors," *Adv. Electr. Electron. Eng.*, vol. 5, pp. 114–119, Jun. 2011.
- [15] K. G. Papadopoulos and N. I. Margaritis, "Extending the symmetrical optimum criterion to the design of PID type-p control loops," *J. Process Control*, vol. 22, no. 1, pp. 11–25, Jan. 2012.

- [16] T. Haggglund, *PID Controllers: Theory, Design, Tuning*. 2nd ed. NC, USA: The Instrumentation, Systems, and Automation Society, 1995.
- [17] S. M. Tripathi, A. N. Tiwari, and D. Singh, "Optimum design of proportional-integral controllers in grid-integrated PMSG-based wind energy conversion system," *Int. Trans. Electr. Energy Syst.*, vol. 26, no. 5, pp. 1006–1031, May 2016.
- [18] Y.-S. Kim, I.-Y. Chung, and S.-I. Moon, "Tuning of the PI controller parameters of a PMSG wind turbine to improve control performance under various wind speeds," *Energies*, vol. 8, no. 2, pp. 1406–1425, Feb. 2015.
- [19] M. Alizadeh and S. S. Kojori, "Augmenting effectiveness of control loops of a PMSG (permanent magnet synchronous generator) based wind energy conversion system by a virtually adaptive PI (proportional integral) controller," *Energy*, vol. 91, pp. 610–629, Nov. 2015.
- [20] L. Pan and C. Shao, "Wind energy conversion systems analysis of PMSG on offshore wind turbine using improved SMC and extended state observer," *Renew. Energy*, vol. 161, pp. 149–161, Dec. 2022.

